

A comparison of the hard *ASCA* spectral slopes of broad and narrow-line Seyfert 1 galaxies

W.N. Brandt, S. Mathur and M. Elvis

Harvard-Smithsonian Center for Astrophysics, 60 Garden Street, Cambridge, Massachusetts 02138, USA

23 September 2018

ABSTRACT

The soft (≈ 0.1 – 2.0 keV) X-ray spectra of narrow-line Seyfert 1 galaxies are known to be generally steeper than those of Seyfert 1 galaxies with broader optical permitted lines. This has been attributed to the presence of strong soft X-ray excesses, over the hard X-ray power law, in many narrow-line Seyfert 1s. Here we use the currently available *ASCA* data to systematically compare the harder (≈ 2 – 10 keV) X-ray continua of soft *ROSAT* narrow-line Seyfert 1s with those of Seyfert 1s with larger $H\beta$ FWHM. Our robust and nonparametric testing suggests, with high statistical significance, that soft *ROSAT* narrow-line Seyfert 1s have generally steeper intrinsic hard X-ray continua than Seyfert 1s with larger $H\beta$ FWHM. The hard photon index trend appears similar to the previously known soft photon index trend, although with a reduced photon index spread. If the soft X-ray excesses of all Seyfert 1s are confined to below ≈ 1 keV they cannot directly affect the ≈ 2 – 10 keV spectra studied here. However, as suggested for the extreme narrow-line Seyfert 1 RE J 1034+393, a strong soft X-ray excess may affect the accretion disc corona which creates the underlying hard X-ray power law. If this is occurring, then more detailed study of this physical process could give clues about the formation of the underlying continua of all Seyferts. Other effects, such as intrinsic 2–10 keV continuum curvature, could also lead to the observed photon index trend and need further study.

Key words: galaxies: active – X-rays: galaxies.

1 INTRODUCTION

The X-ray spectra of most Seyfert 1 type galaxies are formed predominantly within ~ 50 Schwarzschild radii of their black holes, while Seyfert optical permitted lines are formed in a separate and significantly larger region. Thus, it was remarkable when an extremely strong anticorrelation was found between *ROSAT* spectral softness and $H\beta$ full width at half-maximum intensity (FWHM) in type 1 Seyferts (e.g. Boller, Brandt & Fink 1996, hereafter BBF96) and quasars (e.g. Laor et al. 1994; Laor et al. 1997). Ultrasoft narrow-line Seyfert 1 galaxies (hereafter NLS1; see Osterbrock & Pogge 1985, Goodrich 1989 and Stephens 1989) represent one extreme of this anticorrelation and can often have *ROSAT* photon indices, from simple power-law fits, exceeding 3. Such steep spectra appear to be due to strong soft X-ray excesses (compared to the underlying X-ray power law) in the *ROSAT* band below about 1 keV. These soft X-ray excesses show rapid and large amplitude variability, supporting a compact origin. NLS1 also tend to lie towards the strong Fe II, weak [O III] extreme of the first Boroson & Green

(1992) eigenvector, and for this reason they are sometimes called I Zw 1 objects.

Comparatively little is known about the harder X-ray properties of NLS1, although *ASCA* (Tanaka, Inoue & Holt 1994) observations of a few ultrasoft NLS1 have shown that they can have interesting spectral differences from more typical Seyfert 1s. For example, Pounds, Done & Osborne (1995, hereafter PDO95) found a power law with a remarkably large 2–10 keV *ASCA* photon index of $\Gamma \approx 2.6$ in the *ROSAT* Wide Field Camera NLS1 RE J 1034+393. They also confirmed the presence of a strong soft X-ray excess above the steep power law (also see Puchnarewicz et al. 1995). This soft excess dominates the X-ray spectrum at energies $\lesssim 1$ keV. PDO95 drew an analogy between RE J 1034+393 and Galactic black hole candidates accreting in their ultrasoft high states. They also suggested that its intense soft X-ray flux may be cooling its accretion disc corona to cause the anomalously steep hard X-ray spectrum (see section 7 of Maraschi & Haardt 1997). It is important to determine if other ultrasoft NLS1 also show steep 2–10 keV spectra (see Pounds &

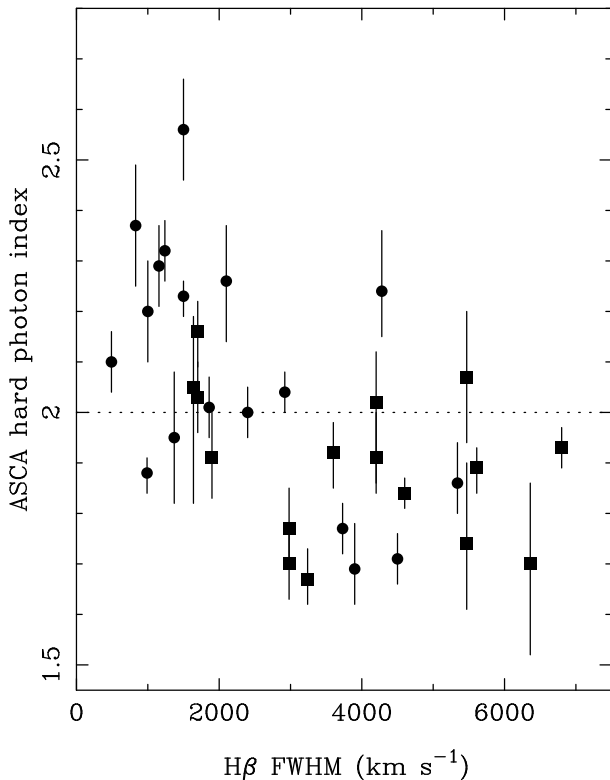


Figure 1. Plot of *ASCA* hard X-ray photon index versus full width at half-maximum intensity of the $H\beta$ line for Seyfert 1 type galaxies. Squares are Seyfert 1s from N97, and dots are other Seyfert 1s from the literature (see the text for details). The dotted line at $\Gamma = 2$ is drawn for illustrative purposes.

Brandt 1997), as this could give much needed clues about the formation of the underlying continua of all Seyferts.

In this letter we use the currently available *ASCA* data to compare the ≈ 2 –10 keV intrinsic power-law slopes of NLS1 with soft *ROSAT* spectra to those of Seyfert 1s with larger $H\beta$ FWHM. We are interested in the *intrinsic* slopes (free from effects such as Compton reflection) since these are thought to probe the fundamental nature of the underlying hard X-ray continuum. As is standard practice, we quantify spectral slopes using power-law photon indices, and power laws usually appear to be reasonable representations of the *intrinsic* 2–10 keV continua, at least to first order.

2 SPECTRAL SLOPE COMPARISON

2.1 Selection of objects under consideration

Figure 1 shows a plot of *ASCA* hard (≈ 2 –10 keV) photon index versus the FWHM of the $H\beta$ line. This plot may be compared with the analogous plots made using lower-energy *ROSAT* data shown as figure 8 of BBF96 and figure 5a of Laor et al. (1997). We have only used *ASCA* X-ray data to make this diagram to avoid calibration uncertainties between different satellites. We have only used data above

2 keV to avoid possible confusion by soft X-ray excesses, cold absorbers, warm absorbers and other low-energy spectral complexity.

2.1.1 The Nandra et al. (1997) Seyfert 1s

The squares in Figure 1 are Seyfert 1s from the large sample recently presented by Nandra et al. (1997, hereafter N97). We have used the photon indices from table 6 of N97. These are for the 3–10 keV band. The effects of Compton reflection have been included in the fitting, and this tends to increase the derived intrinsic photon indices by $\Delta\Gamma \approx 0.12$. Appropriate modelling of the iron $K\alpha$ emission line has also been performed, although the derived photon indices are not sensitive to details of the line model (see section 4.3 of N97). The 3–10 keV photon indices are expected to be very similar to the 2–10 keV photon indices (K. Nandra, private communication), and explicit spectral fitting of several of the N97 objects verifies that this appears to be the case.

All objects in N97 are included in Figure 1 except for NGC 4151, NGC 6814 and 3C 120. We have excluded NGC 4151 due to its complex spectrum in the *ASCA* band which hinders a precise determination of its intrinsic photon index (see Weaver et al. 1994 and references therein) as well as its strong optical line profile changes (e.g. Penston & Pérez 1984). We have excluded NGC 6814 because it does not have measured photon indices in most of the tables of N97 (due to its faintness) and also because it shows persistent and strong optical line variability (e.g. Sekiguchi & Menzies 1990). We have excluded 3C 120 because it is radio loud and has superluminal motion. We have not used the N97 results for NGC 4051 or Mrk 766, and we discuss these two objects in more detail below. Three objects in the N97 sample were observed by *ASCA* twice (MCG–6–30–15, Mrk 841 and NGC 3783), and we have used all six of these *ASCA* measurements in our analysis. Our statistical results below do not materially change if we systematically use only the flattest, only the steepest, or the averaged N97 photon indices for these three objects. The N97 sample is composed of well-studied, hard X-ray bright Seyfert 1s, as these were the Seyfert 1s predominantly observed during early *ASCA* observations. It is biased against soft *ROSAT* NLS1 at some level. NGC 4051 and Mrk 335, the two objects in the N97 sample with the smallest $H\beta$ FWHM, have their similarities to NLS1 discussed in section 5.1 of BBF96.

We have verified that radio-loud objects, which generally have flatter X-ray spectra than radio-quiet objects, are not affecting the trend shown in Figure 1. The N97 objects with large $H\beta$ FWHM are ‘typical’ radio-quiet Seyfert 1 galaxies such as NGC 3227, NGC 3516, NGC 3783, NGC 5548 and Fairall 9.

2.1.2 Other Seyfert 1s and low-luminosity Seyfert 1 type quasars

The solid dots in Figure 1, from left to right, show the 2–10 keV *ASCA* photon indices for IRAS 17020+4544 (Brandt et al., in preparation), PG 1244+026 (Fiore et al., in preparation), NGC 4051 (Guainazzi et al. 1996), H 0707–495 (Hayashida 1997 and independent fitting), NAB 0205+024 (Fiore et al., in preparation), I Zw 1 (Hayashida 1997),

Mrk 478 (Madejski et al., in preparation), RE J 1034+393 (PDO95), PKS 0558–504 (Brandt et al., in preparation), PG 1211+143 (Yaqoob et al. 1994 and independent fitting), IRAS 13349+2438 (Brinkmann et al. 1997 and independent fitting), Mrk 766 (Leighly et al. 1996), PG 1116+215 (Nandra et al. 1996 and independent fitting), ESO 141–G55 (Reynolds 1997 and independent fitting), Mrk 1040 (Reynolds 1997 and independent fitting), RX J 0437–470 (Wang et al. 1997 and independent fitting), MR 2251–178 (Reynolds 1997 and independent fitting) and Mrk 290 (table 2 of Turner et al. 1997). Iron line modelling has been included in the fitting when appropriate (see the cited references for details). As with the N97 Seyfert 1s, the photon indices for these objects do not appear to be sensitive to the details of the iron line modelling.

The intrinsic hard photon indices of NGC 4051 and Mrk 766 appear to be variable. For NGC 4051, we have used the photon index from the time averaged analysis in section 4.3 of Guainazzi et al. (1996). This photon index appears to provide a reasonable description of the typical source behaviour (see figure 12 of Guainazzi et al. 1997). For Mrk 766, Leighly et al. (1996) state that the 2–10 keV photon index varies abruptly between $1.57_{-0.07}^{+0.07}$ and $2.00_{-0.04}^{+0.03}$ when the source changes from a low state to a high state. The time averaged value is likely to be closer to 2.00 than 1.57 (see Leighly et al. 1996 for details), and table 2 of N97 gives a time averaged value of $2.00_{-0.05}^{+0.05}$ (a similar value is obtained by Hayashida 1997). We adopt this value and show below that our statistical results are not sensitive to the precise photon index adopted for Mrk 766. All results discussed below should be implicitly taken to pertain to time averaged Seyfert 1 behaviour, although most of the Seyfert 1s in our sample did not show strong photon index variability during their *ASCA* observations.

Figure 1 does not include the radio-loud objects from Reynolds (1997) or highly luminous quasars (with 2–10 keV luminosities larger than 1×10^{45} erg s⁻¹) as our interest here is in radio-quiet Seyfert 1 galaxies. We have not used NGC 2992 (a narrow emission line galaxy with internal absorption; NELG) from the Reynolds (1997) sample, due to the fact that its intrinsic photon index is not well determined by the *ASCA* data (see Weaver et al. 1996; also see Section 1 for an explanation of why we are only interested in intrinsic photon indices). The 2–10 keV spectrum of NGC 2992 is strongly influenced by a time-delayed Compton reflection continuum and other complexities which obscure the true shape of the underlying continuum. We have not plotted the NLS1 IRAS 13224–3809 (see Boller et al. 1993) in Figure 1 due to the fact that its 2–10 keV spectral shape appears to be highly variable and is poorly constrained by current data (see table 4.4.1 of Otani 1995). Its hard X-ray photon index appears to vary between roughly 1.3–2.3, although the precise values obtained depend on details of the modelling. For comparison with Figure 1, IRAS 13224–3809 has an H β FWHM of ≈ 650 km s⁻¹, and Hayashida (1997) gives a time averaged hard photon index of 2.15 ± 0.13 .

2.1.3 Selection effects

While the objects in Figure 1 are not drawn from a rigorously defined complete sample, we have used all the currently available radio-quiet Seyfert 1s with reliably measured

intrinsic ASCA photon indices in an attempt to avoid any biases. There are 34 data points in Figure 1.

One possible selection effect is that several of the NLS1 that have been observed with *ASCA* have been chosen as targets due to their soft spectra in the *ROSAT* band. This does not invalidate comparisons made using the data in Figure 1, but it does restrict our comparison to that of soft *ROSAT* spectra NLS1 versus Seyfert 1 galaxies with larger H β FWHM. This is to be understood in all discussion below. If the *ROSAT* Γ versus H β FWHM correlation, after correction for possible absorption effects in the *ROSAT* band, is as tight as suggested by figure 5a of Laor et al. (1997), then a distinction between soft *ROSAT* NLS1 and NLS1 more generally may be unimportant.

Seyfert 1 galaxies with both *ROSAT* photon indices larger than 3 as well as H β FWHM larger than 3000 km s⁻¹ appear to be strongly discriminated against by nature (see Section 1; Pounds & Brandt 1997 give the clearest illustration of this effect so far). Thus the lack of *ASCA* observations of Seyfert 1s with both large H β FWHM and *ROSAT* photon indices larger than 3 is not an artificial selection bias, but is rather due to a real and physically interesting effect.

2.2 Statistical comparisons

Examination of Figure 1 suggests that NLS1 with soft *ROSAT* spectra have $\Gamma_{\text{Hard}} > 2$ more frequently than Seyfert 1s with larger H β FWHM. Below we perform statistical tests to quantify the significance of the apparent trend in Figure 1.

2.2.1 Definition of samples

Some of the statistical tests below are designed to compare two samples of objects. Therefore, we have divided the Seyfert 1s in Figure 1 into two samples. The first sample (hereafter NL for ‘narrow lines’) is composed of the objects with H β FWHM smaller than 2000 km s⁻¹. The second sample (hereafter BL for ‘broad lines’) is composed of the objects with H β FWHM larger than 2000 km s⁻¹. We have chosen the 2000 km s⁻¹ dividing value of H β FWHM based on the a priori definition for NLS1 given in section IVb of Stephens (1989). However, we have included IRAS 13349+2438 in NL rather than BL. As discussed in section 4.5 of Brandt, Fabian & Pounds (1996), which was written before the *ASCA* results were available, IRAS 13349+2438 has many striking similarities to NLS1. In addition to its rather narrow Balmer lines (it has an H β FWHM of 2100 km s⁻¹), IRAS 13349+2438 has a soft *ROSAT* spectrum, strong optical Fe II emission and weak forbidden line emission (see Wills et al. 1992). As our goal below is to compare the *ASCA* hard photon index distributions of soft *ROSAT* NLS1 and Seyfert 1s with larger H β FWHM, inclusion of IRAS 13349+2438 in NL is clearly warranted. We show later that our conclusions do not depend on the treatment of IRAS 13349+2438. In total, we have 15 photon indices in NL and 19 photon indices in BL.

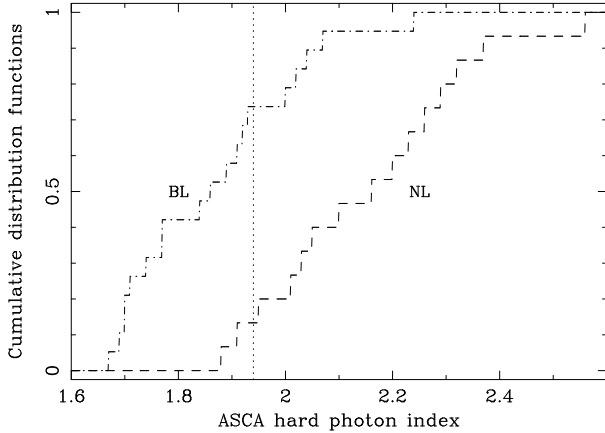


Figure 2. Cumulative distribution functions for the photon indices of NL and BL. The vertical dotted line shows the value of the photon index at which the Kolmogorov-Smirnov D statistic is obtained.

2.2.2 Statistical tests

We first performed a two-sample Kolmogorov-Smirnov test to determine the probability that NL and BL were drawn from the same parent distribution function. This test is robust and nonparametric, although it does not provide formal information as to why two distributions are different (i.e. they could differ in mean, variance, skewness or some other property, but the Kolmogorov-Smirnov test does not discriminate between these possibilities). NL and BL are large enough for the Kolmogorov-Smirnov test to be applicable (see equation 14.3.10 of Press et al. 1992 and Stephens 1970). We obtain a Kolmogorov-Smirnov statistic of $D = 0.604$, and in Figure 2 we plot the cumulative distribution functions for NL and BL used by the Kolmogorov-Smirnov test. Given the value of D we find that NL and BL have less than a 0.25 per cent chance of being drawn from the same parent distribution function, and Figure 2 suggests that the main reason for the low probability is likely to be a difference in the central photon indices of NL and BL.

In order to obtain more descriptive information about the differences between NL and BL, we have calculated some of their moments. The mean photon index of NL is 2.15, the variance of the NL photon indices is 0.036 and the standard error of the NL mean is 0.049. The mean photon index of BL is 1.87, the variance of the BL photon indices is 0.025 and the standard error of the BL mean is 0.036. Note that the NL mean photon index is $\gtrsim 5$ standard errors larger than the BL mean photon index.

We have used Student's t -test (for distributions with nonequal variances; see Press et al. 1992) to examine whether NL and BL have significantly different means. We obtain a t value of 4.73. There is less than a 0.02 per cent chance that t could be this large or larger, for distributions with equal means. While Student's t -test is a parametric test and is subject to the limitations described in chapter 3 of Siegel (1956), we nevertheless consider the large value of t to be suggestive.

We have performed a Spearman rank-order correlation

using the data shown in Figure 1. This test is sensitive to any monotonic relation between two variables and is more general than Pearson's r -test. As described in detail in Siegel (1956), it is nonparametric, robust and requires far fewer assumptions than parametric tests. It also does not require the division of the objects into NL and BL (this division is somewhat artificial if there is a continuous trend present in Figure 1). We have checked our implementation of the Spearman test using data from Laor et al. (1997), and we obtain entirely consistent results. Using the data in Figure 1, we obtain a Spearman r_s value of -0.583 . The Spearman probability associated with this r_s value is 3×10^{-4} (that is, there is less than a 0.1 per cent chance of obtaining a Spearman r_s value with this large a magnitude by chance). Thus, the Spearman rank-order correlation indicates that there is a highly significant anticorrelation between H β FWHM and ASCA hard photon index for the objects in Figure 1.

2.2.3 Safety checks

We have performed several safety checks to examine the reliability of our statistical results. First of all, we have verified that they do not depend on any single data point in Figure 1. This is understandable since the Kolmogorov-Smirnov and Spearman tests we have employed are relatively insensitive to outlying points. For example, we still find strong evidence for an anticorrelation even if the most extreme NLS1 illustrated, RE J 1034+393, is neglected. Running the Spearman rank-order correlation without RE J 1034+393, we obtain an r_s value of -0.566 and a Spearman probability of 6×10^{-4} . However, there is no known reason why RE J 1034+393, or any other object in Figure 1, should be neglected.

Conservatively using the flat photon index for Mrk 766 from section 4.1 of Leighly et al. (1996) does not change our basic statistical results. Using the flat photon index, we obtain $r_s = -0.549$ and a Spearman probability of 8×10^{-4} . We have also verified that the inclusion of NGC 2992 or IRAS 13224-3809 (see Section 2.1.2) does not change our basic statistical conclusions. Including IRAS 13349+2438 in BL rather than NL does not affect the anticorrelation, because the Spearman analysis does not depend on the division into NL and BL.

If we use the hard photon indices from table 4 of N97, which do not include Compton reflection in the spectral fitting, the trend suggested above is not affected. In fact, it becomes statistically stronger because all the squares in Figure 1 shift downward (on the average by $\Delta\Gamma = -0.12$).

As the photon indices in Figure 1 have errors associated with them, we have performed Monte-Carlo simulations to verify that it is not just a chance realization of the best-fitting photon index values that leads to the apparent anticorrelation. In these simulations we generate sets of photon indices based on the data points and errors in Figure 1, and we then perform Spearman rank-order correlations using these sets. We generate the photon indices from Gaussian distributions centred on the points in Figure 1, and we follow the conservative prescriptions in section 2.1 of N97 regarding the translation of confidence limits into Gaussian 1σ values. In 94.0 per cent of the simulations, we can rule out a chance anticorrelation with greater than 99 per cent confidence. In 99.7 per cent of the simulations, we can rule out a chance anticorrelation with greater than 95 per cent

confidence. Note that the 95 per cent confidence level stated here does not mean that we have weakened our threshold for correlation testing. It is only used to describe the (in itself unlikely) tail of the distribution of Spearman probabilities that arises from our Monte Carlo calculations. It is unlikely that our statistical results are due to a chance realization of the best fitting photon index values.

3 DISCUSSION

The currently available data suggest, with high statistical significance, that soft *ROSAT* NLS1 have generally steeper 2–10 keV intrinsic spectral slopes than Seyfert 1s with larger $H\beta$ FWHM. Note that this is a robust statistical statement regarding two populations, and that the discovery of a single discrepant Seyfert 1 is unlikely to alter it.

The trend suggested by Figure 1 appears similar to the well-established *ROSAT* $\Gamma/H\beta$ FWHM trend, although the range of photon indices in Figure 1 (≈ 1.6 – 2.6) is about half that seen in lower-energy *ROSAT* data (≈ 1.9 – 4.2). Soft excesses probably lead to the larger photon index dispersion observed in the *ROSAT* band. However, soft excesses are thought to be confined to below about 1 keV. Figure 1 uses no data below 2 keV, and thus the hard photon index trend illustrated there would probe different and new Seyfert physics. As discussed by PDO95, photons from the soft excesses of ultrasoft NLS1 could Compton cool the coroneae which create their harder flux and thereby steepen their 2–10 keV continua (also see Maraschi & Haardt 1997). If this is indeed the cause of the observed effect, then comparative studies of soft *ROSAT* NLS1 and Seyfert 1s with broader permitted lines will have provided one of the first direct illustrations of a physical process that influences the origin of the underlying hard X-ray continua from Seyfert galaxies. Other possibilities, such as significant curvature in the underlying 2–10 keV continua of some Seyfert 1s, also need further examination (for a detailed study see Brandt et al., in preparation).

Some researchers have considered models for NLS1 in which they are Seyfert 1s viewed along a particular line of sight (e.g. highly pole-on; Osterbrock & Pogge 1985; Puchnarewicz et al. 1992), although such models appear to have trouble explaining all the known optical line (e.g. Boroson 1992; but also see Hes, Barthel & Fosbury 1993 for evidence that [O III] may not be isotropic) and X-ray properties. If, despite current indications, a special orientation does turn out to be the root cause of NLS1 properties then the hard photon index trend described here would require the hard power-law shapes of Seyfert 1s to be orientation dependent.

Additional *ASCA* analyses of NLS1 (e.g. Ton S 180, RX J 0148–27 and IRAS 20181–2244) are needed to further study the hard photon index trend suggested here. They will thereby probe the full range of Seyfert 1 spectral shapes (cf. Elvis 1992) and clarify the extent to which historical and other selection effects have influenced measurements of the dispersion of Seyfert 1 hard X-ray slopes. It would also be of great interest to see if an analogous trend is found in higher luminosity Seyfert 1 type quasars. The Laor et al. (1997) sample is an obvious one in which to search for such a trend, although it may not have enough ultrasoft quasars

to provide definitive results. There are only three quasars in Laor et al. (1997) with best fit *ROSAT* photon indices larger than 3, and one of these is faint and unlikely to yield precise *ASCA* spectral parameters.

ACKNOWLEDGMENTS

We gratefully acknowledge financial support from the Smithsonian Institution (WNB) and NASA grant NAGW-4490 (SM). We thank F. Fiore for communicating two photon indices prior to publication. We thank C. Done, A. Fabian, F. Fiore, J. Halpern, A. Laor, K. Nandra, R. Pogge, C. Reynolds and B. Wilkes for helpful discussions.

REFERENCES

- Boller Th., Trümper J., Molendi S., Fink H., Schaeidt S., Caulet A., Dennefeld M., 1993, *A&A*, 279, 53
 Boller Th., Brandt W.N., Fink H., 1996, *A&A*, 305, 53
 Boroson T.A., 1992, *ApJ*, 399, L1
 Boroson T.A., Green R.F., 1992, *ApJS*, 80, 109
 Brandt W.N., Fabian A.C., Pounds K.A., 1996, *MNRAS*, 278, 326
 Brinkmann W., Kawai N., Ogasaka Y., Siebert J., 1997, *A&A*, 316, L9
 Elvis M., 1992, in Tanaka Y., Koyama K., eds, *Frontiers of X-ray Astronomy*. Universal Acad. Press, Tokyo, p. 567
 Goodrich R.W., 1989, *ApJ*, 342, 224
 Guainazzi M., Mihara T., Otani C., Matsuoka M., 1997, *PASJ*, in press
 Hayashida K., 1997, in Peterson B.M., Cheng F.-Z., Wilson A.S., eds, *Emission Lines in Active Galaxies: New Methods and Techniques*. Astronomical Society of the Pacific Press, San Francisco, p. 40
 Hes R., Barthel P.D., Fosbury R.A.E., 1993, *Nature*, 362, 326
 Laor A., Fiore F., Elvis M., Wilkes B.J., McDowell J.C., 1994, *ApJ*, 435, 611
 Laor A., Fiore F., Elvis M., Wilkes B.J., McDowell J.C., 1997, *ApJ*, in press
 Leighly K.M., Mushotzky R.F., Yaqoob T., Kunieda H., Edelson R., 1996, *ApJ*, 469, 14
 Maraschi L., Haardt F., 1997, in Wickramasinghe D., Ferrario L., Bicknell G., eds, *IAU Coll. 163: Accretion Phenomena and Related Outflows*. Pub. Astr. Soc. of Australia Press, Sydney, in press
 Nandra K., George I.M., Turner T.J., Fukazawa Y., 1996, *ApJ*, 464, 215
 Nandra K., George I.M., Mushotzky R.F., Turner T.J., Yaqoob T., 1997, *ApJ*, in press (N97)
 Osterbrock D.E., Pogge R.W., 1985, *ApJ*, 297, 166
 Otani C., 1995, PhD thesis, University of Tokyo
 Penston M.V., Pérez E., 1984, *MNRAS*, 211, 33P
 Pounds K.A., Done C., Osborne J., 1995, *MNRAS*, 277, L5 (PDO95)
 Pounds K.A., Brandt W.N., 1997, in Makino F., Mitsuda K., eds, *X-Ray Imaging and Spectroscopy of Cosmic Hot Plasmas: ASCA Third Anniversary Proceedings*. Univ. Acad. Press, Tokyo, in press
 Press W.H., Teukolsky S.A., Vetterling W.T., Flannery B.P., 1992, *Numerical Recipes in Fortran: Second Edition*. Cambridge University Press, Cambridge
 Puchnarewicz E.M., Mason K.O., Córdova F.A., Kartje J., Branduardi-Raymont G., Mittaz J.P.D., Murdin P.G., Allington-Smith J., 1992, *MNRAS*, 256, 589
 Puchnarewicz E.M., Mason K.O., Siemiginowska A., Pounds K.A., 1995, *MNRAS*, 276, 20

- Reynolds C.S., 1997, MNRAS, in press
Sekiguchi K., Menzies J.W., 1990, MNRAS, 245, 66
Siegel S., 1956, Nonparametric Statistics for the Behavioral Sciences. McGraw Hill, New York
Stephens M.A., 1970, Journal of the Royal Statistical Society, 32, 115
Stephens S.A., 1989, AJ, 97, 10
Tanaka Y., Inoue H., Holt S.S., 1994, PASJ, 46, L37
Turner T.J., George I.M., Kallman T., Yaqoob T., Życki P.T., 1997, ApJ, in press
Wang T., Otani C., Cappi M., Matsuoka M., Brinkmann W., Leighly K., 1996, MNRAS, in press
Weaver K.A., Yaqoob T., Holt S.S., Mushotzky R.F., Matsuoka M., Yamauchi M., 1994, ApJ, 436, L27
Weaver K.A., Nousek J., Yaqoob T., Mushotzky R.F., Makino F., Otani C., 1996, ApJ, 458, 160
Wills B.J., Wills D., Evans N.J., Natta A., Thompson K.L., Breger M., Sitko M.L., 1992, ApJ, 400, 96
Yaqoob T., Serlemitsos P., Mushotzky R.F., Madejski G., Turner T.J., Kunieda H., 1994, PASJ, 46, L173

This paper has been produced using the Royal Astronomical Society/Blackwell Science L^AT_EX style file.